

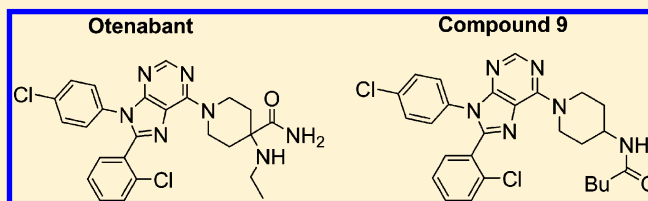
## Peripherally Selective Diphenyl Purine Antagonist of the CB1 Receptor

Alan Fulp, Katherine Bortoff, Yanan Zhang, Rodney Snyder, Tim Fennell, Julie A. Marusich, Jenny L. Wiley, Herbert Seltzman, and Rangan Maitra\*

Discovery Sciences, Research Triangle Institute, 3040 Cornwallis Road, P.O. Box 12194, Research Triangle Park, North Carolina 27709, United States

## Supporting Information

**ABSTRACT:** Antagonists of the CB1 receptor can be useful in the treatment of several important disorders. However, to date, the only clinically approved CB1 receptor antagonist, rimonabant, was withdrawn because of adverse central nervous system (CNS)-related side effects. Since rimonabant's withdrawal, several groups are pursuing peripherally selective CB1 antagonists. These compounds are expected to be devoid of undesirable CNS-related effects but maintain efficacy through antagonism of peripherally expressed CB1 receptors. Reported here are our latest results toward the development of a peripherally selective analog of the diphenyl purine CB1 antagonist otenabant **1**. Compound **9** (*N*-{1-[8-(2-chlorophenyl)-9-(4-chlorophenyl)-9*H*-purin-6-yl]piperidin-4-yl}pentanamide) is a potent, orally absorbed antagonist of the CB1 receptor that is >50-fold selective for CB1 over CB2, highly selective for the periphery in a rodent model, and without efficacy in a series of *in vivo* assays designed to evaluate its ability to mitigate the central effects of  $\Delta^9$ -tetrahydrocannabinol through the CB1 receptor.



## INTRODUCTION

The cannabinoid receptors CB1 and CB2 are G-protein-coupled receptors (GPCRs) that primarily function as activators of inhibitory G proteins (Gi/o).<sup>1</sup> CB1 receptors are expressed widely throughout the body; however, they are most heavily expressed in the central nervous system (CNS). CB2 receptors are found most abundantly in the periphery. Both receptors belong to an endocannabinoid system (ECS) that regulates many physiological systems and can be targeted to treat several serious disorders. Currently, various components of the ECS are under evaluation for the treatment of pain, inflammation, obesity, liver disease, and diabetes.<sup>2,3</sup>

For example, the antagonism of CB1 has been investigated for the treatment of metabolic disorders such as diabetes and obesity. Past translational research in this regard led to the clinical approval of rimonabant (SR141716A) for weight loss in Europe. Rimonabant is a potent and selective CB1 receptor inverse agonist/antagonist. Regrettably, rimonabant produced serious side effects such as depression, anxiety, and suicidal ideation in a subset of patients. These CNS-related side effects led to the withdrawal of rimonabant from European markets, and the drug was not approved for use in the United States.<sup>4,5</sup> Several other CB1 antagonists, such as otenabant (**1**) (Figure 1), taranabant, and ibipinabant, were pulled from clinical development upon discovery of rimonabant's CNS-related side effects.<sup>6</sup>

A possible strategy to avoid CNS-related side effects is to generate CB1 antagonists that do not cross the blood-brain barrier (BBB) and have low brain penetration. Generally, compounds that have <10% brain penetration are considered

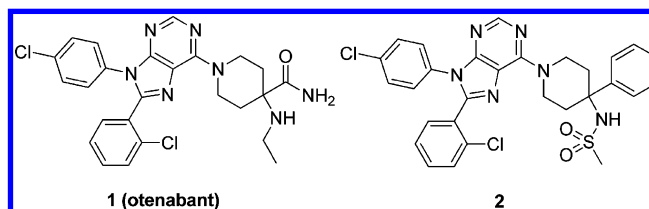


Figure 1. Otenabant and a peripherally selective analogue.

peripherally selective. In rodent studies, compounds that have <5% brain penetration in unperfused tissue samples are considered peripherally restricted because the volume of blood in a rodent brain accounts for ~3–6% of its total weight.<sup>7,8</sup> Efforts are underway to produce peripherally restricted CB1 antagonists are ongoing.<sup>9</sup> Our group has focused on **1** as a starting point for further optimization.<sup>10</sup> Despite being nontissue selective, **1** has several properties that could be optimized to produce peripherally selective compounds, including a formula weight of 510, a topological polar surface area (TPSA) of 102, and 3 H-bond donors.<sup>11</sup> However, intramolecular H bonding effectively lowers the polarity of **1**, allowing for penetration into the CNS.<sup>11</sup> In our initial publication, we reported several diphenyl purines with formula weights and TPSA similar to **1** but lacking the ability to form intramolecular H bonds. To that end, we were able to discover **2**, an analogue of **1** that has a formula weight of 593 and a TPSA 101.<sup>10</sup> However, unlike **1**, **2** is a peripherally selective

Received: July 25, 2013

compound. Oral dosing of **2** at 10 mg/kg in Sprague–Dawley (SD) rats showed good oral absorption ( $C_{\max} = 1653$  ng/g) and limited penetration into the CNS (brain-to-plasma ratios of 0.05–0.11 were observed).<sup>12</sup>

On the basis of these promising results with **2**, we investigated a series of analogues with substitutions at the 4-amino position of **3** (Figure 2) in an attempt to further limit

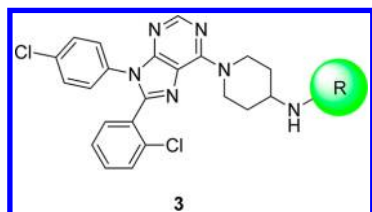


Figure 2. General strategy for compound development.

CNS penetration. Although the 4-amino-4-phenyl piperidine portion of **2** was the most potent amino piperidine tested in our previous studies, these efforts focused on the 4-amino piperidine moiety of structure **3** because of its lower formula weight; **3** allows us to add steric bulk while maintaining the formula weight <600.

## RESULTS

**Ligand Design and Synthesis.** Of the compounds evaluated in our earlier studies that lacked additional substitution on the piperidine ring, the 4-amino piperidine compounds (represented by structure **3**) were the most potent analogues.<sup>10</sup> However, only a limited number of R groups were tested. In this study, a number of different R-group substitutions were targeted to augment our understanding of the existing structure–activity relationship (SAR). Carbamates, amides, and sulfonamides were chosen for further examination because they were previously found to be favored over ureas.<sup>10</sup>

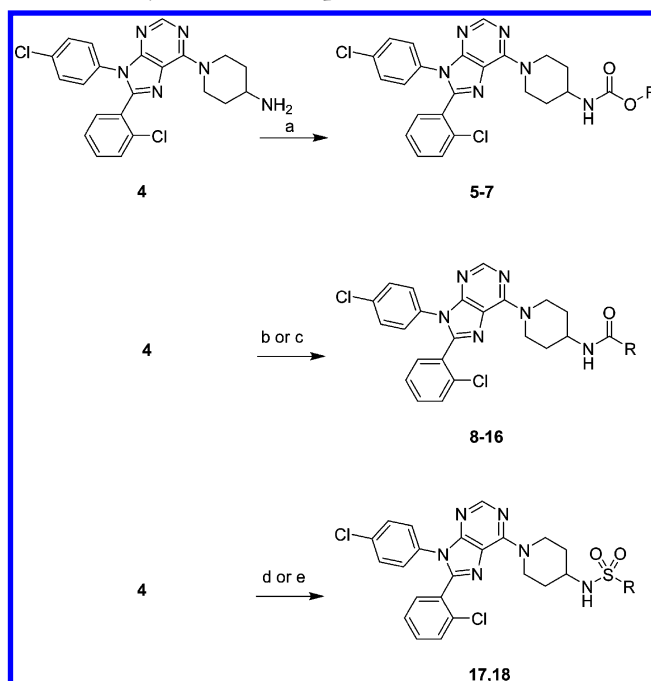
Synthesis of the compounds was accomplished as described in Scheme 1. Carbamates were made by reacting the previously described amine **4**<sup>10</sup> and the appropriate chloroformate. Amides **7–16** were synthesized from **4** using benzotriazol-1-yloxy)tris(dimethylamino)phosphonium hexafluorophosphate (BOP), triethylamine, and the appropriate amine or acid. Sulfamide **17** was synthesized by heating **4** with sulfamide in dioxane. Sulfonamide **18** was prepared by reacting **4**, triethylamine, and trifluoromethanesulfonic anhydride in dichloromethane.

**Pharmacological Characterization.** Compounds were tested in vitro for antagonist activity at CB1 using a calcium mobilization assay. This CB1-antagonist activity is expressed as an apparent dissociation affinity constant ( $K_e$ ).<sup>13</sup> Compounds that had  $K_e$  of <10 nM were assessed for their selective affinity for CB1 versus CB2 receptors, as determined using a [<sup>3</sup>H]CP55940 displacement assay. For each receptor, the values were expressed as the equilibrium dissociation constant ( $K_i$ ).<sup>10</sup> Selectivity was expressed as a ratio of these constants.

In general, excellent activity and potency were observed with these compounds (Table 1). Ten of the 14 compounds had  $K_e$  < 10 nM and  $K_i$  < 20 nM at the CB1 receptor. All compounds tested were found to be selective for the CB1 versus CB2 receptor. Selectivity ranged from ~22-fold for **11** to >4000-fold for **7**.

**Pharmacokinetic Studies of Select Compounds.** Pharmacokinetic (PK) studies were performed with compounds **6** and **9**. These compounds were chosen for several

## Scheme 1. Synthesis of Compounds<sup>a</sup>



<sup>a</sup>Reagents and conditions: (a) appropriate chloroformate, triethylamine (TEA), tetrahydrofuran (THF); (b) appropriate carboxylic acid, benzotriazol-1-yloxy)tris(dimethylamino)phosphonium hexafluorophosphate (BOP), TEA, THF; (c) appropriate amino acid, BOP, TEA, THF; (d) sulfamide, dioxane, 80 °C; (e) trifluoromethanesulfonic anhydride, TEA, dichloromethane.

reasons. First, testing compounds with different functional groups could maximize the chances of obtaining a compound with a desirable PK profile. Therefore, one amide and one carbamate were chosen. Second, of the compounds with  $K_e$  < 10 nM and selectivity of >50-fold in each series, **6** and **9** had the lowest molecular weight and clogP value in their respective series. Compound **18** was excluded because of its relatively high formula weight. Finally, the shielding effect of bulk on the R group on polarity of the amide or carbamate functionality was taken into consideration. Excessive steric bulk adjacent to the amide or carbamate could effectively minimize the interaction of polar groups of the molecule with their surroundings, thereby increasing penetration across the BBB.

Both **6** and **9** were initially screened for CNS penetration by oral dosing at 10 mg/kg in Sprague–Dawley (SD) rats. Unperfused brain and plasma samples were collected at 1, 2, 4, 8, and 24 h post dose, and samples were analyzed by LC–MS (data not shown). Brain-to-plasma ratios of **6** ranged from 0.14 to 0.46, representing significant brain penetration (data not shown). Minimal to no penetration into the CNS was observed with **9** (Table 2), with brain to plasma ratios ranging from 0.01 to 0.07. The blood volume of an unperfused rodent brain is ~3–6%.<sup>7,8</sup> Therefore, these PK data indicate that **9** has little to no penetration into the CNS and is peripherally selective.

**In Vivo Evaluation of Central CB1 Antagonism.** Compound **9** was also evaluated for its ability to attenuate the central effects of a CB1 agonist in a series of in vivo tests. In this battery of tests, known as the tetrad assay, a classical CB1 agonist such as  $\Delta^9$ -THC produces the suppression of spontaneous activity, antinociception, hypothermia, and catalepsy. These effects are believed to be mediated by CB1

Table 1. Pharmacological Assessment of Compounds

compound	R	K <sub>e</sub> CB1 (nM)	pA <sub>2</sub>	K <sub>i</sub> CB2 (nM) <sup>a</sup>	K <sub>i</sub> CB1 (nM) <sup>a</sup>	selectivity (CB1/CB2)
5	Me	17.0	7.77			
6	Et	2.3	8.64	3.57	426	119
7	Ph	4.0	8.40	2.55	10649	4176
8	cyclohexyl	3.3	8.48	3.35	835	249
9	<i>n</i> -Bu	4.9	8.31	19.47	1046	54
10	cyclohexylmethyl	2.1	8.68	1.93	2360	1223
11	<i>i</i> -Bu	5.4	8.27	4.01	89.5	22
12	cyclopentyl	0.89	9.05	1.54	60.2	39
13	3-methylbutyl	7.4	8.13	2.67	215	81
14	cyclopentylmethyl	2.9	8.54	2.02	569	282
15	(piperidin-1-yl)ethyl	789.0	6.10			
16	Me <sub>2</sub> NCH <sub>2</sub>	140.0	6.85			
17	NH <sub>2</sub>	2768.0	5.56			
18	CF <sub>3</sub>	1.05	8.98	6.1	4501	738

<sup>a</sup>Displacement was measured using [<sup>3</sup>H]CP55940.

Table 2. In Vivo Pharmacokinetic Evaluation of Compound 9<sup>a</sup>

time (h)	plasma conc. (ng/mL)	brain conc. (ng/mL)	brain/plasma ratio
1	730	24.3	0.03
2	1750	71.5	0.04
4	1565	103	0.07
8	1965	62.5	0.03
24	438	5.35	0.01

<sup>a</sup>Compound 9 was dosed orally at 10 mg/kg in three SD rats per time-point.

receptors in the brain and spinal cord<sup>14</sup> and are blocked by coadministration of rimonabant, a potent and CNS penetrant CB1 antagonist.<sup>14,15</sup>

The effects of 9 on the tetrad were measured in adult ICR mice that were orally dosed with either vehicle or 10 mg/kg of

9 followed 30 min later by an i.v. injection of 30 mg/kg of Δ<sup>9</sup>-THC or vehicle. Spontaneous activity was measured in an automated locomotor-activity chamber where beam breaks recorded horizontal movement. Total amulatory counts for this test are shown in Figure 3A. Antinociception was measured by the latency of mice to withdraw their tails from a warm water bath (55 °C). The results for this assay are expressed as the percent of maximum possible effect (% MPE) and are shown in Figure 3B. Hypothermia was measured by comparing the differences in rectal temperature prior to dosing and post Δ<sup>9</sup>-THC dosing; these results are reported as change of temperature (Δ °C) and are shown in Figure 3C. Finally, catalepsy was measured by placing mice on an elevated ring apparatus and measuring the amount of time each mouse remained motionless during a 5 min period following agonist administration. These data are reported as the percent ring immobility and are shown in Figure 3D. The 30 mg/kg dose of

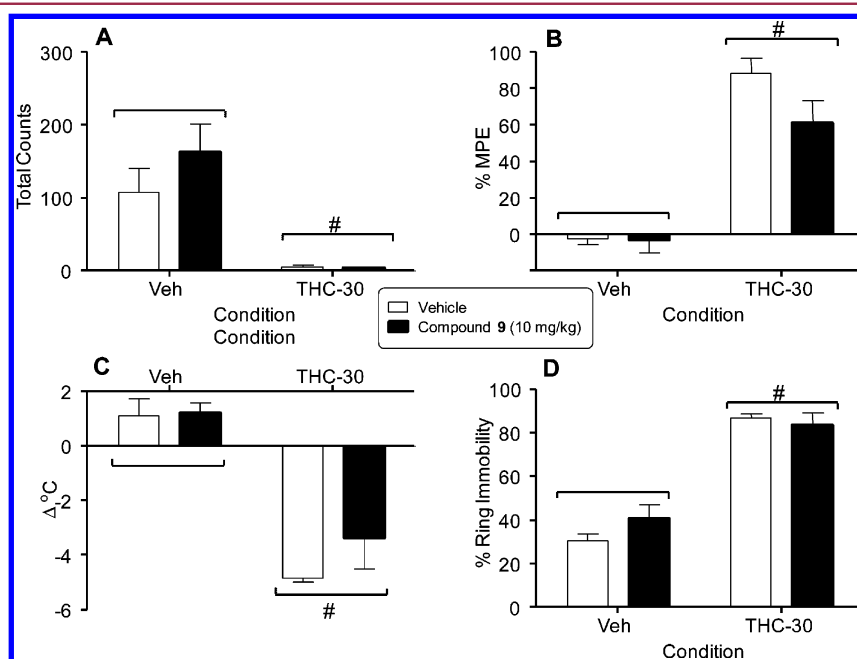


**Figure 3.** Effects of vehicle and Δ<sup>9</sup>-THC (30 mg/kg) tested in combination with vehicle (unfilled bars) or compound 9 (filled bars) on spontaneous activity (A), antinociception (B), rectal temperature (C), and catalepsy (D). Values represent the mean (±SEM) of 5 to 6 mice per group. Pound signs (#) indicate a significant main effect (*p* < 0.05) of Δ<sup>9</sup>-THC (right side of each panel) compared to the vehicle (left side of each panel).

$\Delta^9$ -THC significantly suppressed locomotor activity (panel A) and produced antinociception (panel B), hypothermia (panel C), and catalepsy (panel D), regardless of whether or not **9** was also administered (i.e.,  $p < 0.05$ , main effect of  $\Delta^9$ -THC dose for each measure). Hence, **9** did not reverse any of the cannabimimetic effects of  $\Delta^9$ -THC. It also did not produce any significant effects in these tests by itself when tested in combination with vehicle.

## DISCUSSION

Previous reports indicate that peripherally selective CB1 receptor antagonists have value in treating important diseases such as obesity, diabetes, and liver fibrosis. However, non-tissue-selective compounds that can inhibit CB1 within the CNS have serious adverse effects.<sup>16</sup> Although CB1 is abundantly expressed within the CNS, it is also expressed at lower levels in several peripheral tissues.<sup>1</sup> In contrast, CB2 receptors have limited expression within the CNS but are highly expressed in immune cells and other peripheral tissues.<sup>1</sup> Recent studies also indicate that although CB1 expression in peripheral organs is lower than what is noted within the CNS, this receptor plays an important role in the regulation of metabolic processes. For example, peripheral CB1 receptor inverse agonism reduces obesity by reversing leptin resistance, and hepatic CB1 mediates diet-induced insulin resistance via the inhibition of insulin signaling and clearance in mice.<sup>17,18</sup> Therefore, antagonism of the peripheral CB1 receptor is an attractive strategy to treat cardio-metabolic diseases even though the expression of CB1 is relatively lower in peripheral tissues compared to the CNS.

The goal of these studies was to produce a peripherally selective CB1 antagonist based on **1** as an improvement over our previously reported compound **2** that demonstrated ~10% brain penetration. To achieve this goal, the SAR around **1** was expanded. Several potent ( $K_e$  CB1 <10 nM) and selective (CB2/CB1 >50) amides were identified. Amides **8–14** with a variety of alkyl groups appeared to have significant activity at CB1. However, the presence of basic groups such as piperidine and dimethyl amino was detrimental to activity at CB1, as demonstrated by **15** and **16**. Interestingly, affinity at the CB2 receptor could be modulated by changing the size and shape of the alkyl substituent, as demonstrated by compounds **9–14**. In general, amides with cyclic substituents, such as **8**, **10**, and **14**, had excellent selectivity for CB1 over CB2.

Carbamates **5–7** all had significant activity at the CB1 receptor. However, an order of magnitude increase in activity was observed with the addition of a single methylene to **5** (forming **6**). Aromatic carbamate **7** and ethyl carbamate **6** possessed both good affinity and selectivity. However, phenyl carbamate **7** was an order of magnitude more selective than ethyl carbamate **6** for CB1 over CB2. This result is consistent with the general trend observed for amides with cyclic substituents discussed above.

Sulfamide **17** did not have significant activity in the calcium mobilization assay. Sulfonamide **18** was very active at CB1, and it was very selective for CB1 over CB2. The results for **18** augment our previously reported data for the methanesulfonamide ( $K_e$  CB1 = 71 nM; CB2/CB1  $K_i$  = 37) and the benzenesulfonamide ( $K_e$  CB1 = 0.3 nM; CB2/CB1  $K_i$  = 4888) analogues of **3**.<sup>10</sup> Data for all three sulfonamides of **3** indicated that increased lipophilicity, and to a lesser extent mass, were advantageous for both activity at CB1 and selectivity for CB1 over CB2.

Of the two compounds submitted for PK analyses, only **9** was found to have selectivity for the periphery with brain-to-plasma levels ranging from 0.01 to 0.07. At only one time point did the brain-to-plasma ratio exceed 0.04. A brain-to-plasma ratio of  $\leq 0.06$  in an unperfused rodent brain indicates no discernible penetration into the CNS.<sup>7,8</sup> Thus, **9** is highly selective for the periphery, and this lack of CNS penetration was also confirmed in the tetrad assay wherein the centrally mediated effects of  $\Delta^9$ -THC could not be reversed by **9**.

Reported here are our latest efforts toward the development of a peripherally selective CB1 antagonist for the treatment of a wide range of clinical indications. To date, two peripherally selective analogues of **1** have been identified (**2** and **9**), with **9** representing a significant improvement over **2** in the areas plasma concentration and BBB penetration. Although both compounds are slowly absorbed, plasma levels for **9** are greater than plasma levels of **2** at the  $C_{max}$  (1965 vs 1653 ng/mL) and at the 8 h time point (1965 vs 914 ng/mL).<sup>10</sup> Although **2** has brain-to-plasma ratios that range from 0.05 to 0.11,<sup>10</sup> **9** has brain-to-plasma ratios ranging from 0.01 to 0.07. These data, along with the results from the tetrad, make a compelling case for the peripheral selectivity of **9**. Efficacy studies are currently underway to test the utility of **9** in models of metabolic syndrome and liver disease.

## EXPERIMENTAL SECTION

**Chemistry General.** The purity and characterization of the compounds were established by a combination of the HPLC, TLC, and NMR analytical techniques described below. <sup>1</sup>H and <sup>13</sup>C NMR spectra were recorded on a Bruker Avance DPX-300 (300 MHz) spectrometer and were determined in CDCl<sub>3</sub> or CD<sub>3</sub>OD with tetramethylsilane (TMS) (0.00 ppm) or solvent peaks as the internal reference unless otherwise noted. Chemical shifts are reported in ppm relative to the solvent signal, and coupling constant (*J*) values are reported in hertz (Hz). Thin-layer chromatography (TLC) was performed on EMD precoated silica gel 60 F254 plates, and spots were visualized with UV light or I<sub>2</sub> detection. Low-resolution mass spectra were obtained using a Waters Alliance HT/Micromass ZQ system (ESI). All test compounds were at least 95% pure, as determined by HPLC on an Agilent 1100 system using an Agilent Zorbax SB-Phenyl, 2.1 × 150 mm, 5 μm column with gradient elution using the mobile phases (A) H<sub>2</sub>O containing 0.05% CF<sub>3</sub>COOH and (B) methanol. A flow rate of 1.0 mL/min was used.

**General Procedure for Making Carbamates from 1-[8-(2-Chlorophenyl)-9-(4-chlorophenyl)-9H-purin-6-yl]piperidin-4-amine (**4**).** To a solution of 1-[8-(2-chlorophenyl)-9-(4-chlorophenyl)-9H-purin-6-yl]piperidin-4-amine (**4**) (12.5 mg, 0.028 mmol, 1 equiv) in 2 mL of THF were added triethylamine (0.02 mL, 0.143 mmol, 5 equiv) and the appropriate chloroformate (2 equiv). The reaction was stirred for 16 h. The reaction was concentrated in vacuo. The crude material was purified by silica gel column chromatography using 0–100% ethyl acetate/hexane to yield the pure compound.

**Methyl N-[1-[8-(2-Chlorophenyl)-9-(4-chlorophenyl)-9H-purin-6-yl]piperidin-4-yl]carbamate (**5**).** The reaction proceeded in 79% yield. <sup>1</sup>H NMR (300 MHz, CDCl<sub>3</sub>)  $\delta$  1.44–1.55 (m, 2H), 2.13 (d, *J* = 11.49 Hz, 2H), 3.34 (t, *J* = 12.24 Hz, 2H), 3.68 (br s, 3H), 3.86 (br s, 1H), 4.60 (br s, 1H), 5.40 (br s, 2H), 7.13–7.45 (m, 7H), 7.51 (d, *J* = 6.88 Hz, 1H), 8.38 (s, 1H). [M + H]<sup>+</sup> 497.8.

**Ethyl N-[1-[8-(2-Chlorophenyl)-9-(4-chlorophenyl)-9H-purin-6-yl]piperidin-4-yl]carbamate (**6**).** The reaction proceeded in 55% yield. <sup>1</sup>H NMR (300 MHz, CDCl<sub>3</sub>)  $\delta$  1.25 (t, *J* = 6.92 Hz, 3H), 1.43–1.55 (m, 2H), 2.13 (d, *J* = 11.21 Hz, 2H), 3.34 (t, *J* = 12.01 Hz, 2H), 3.86 (br s, 1H), 4.06–4.22 (m, 2H), 4.58 (br s, 1H), 5.39 (br s, 2H), 7.14–7.43 (m, 7H), 7.51 (d, *J* = 6.69 Hz, 1H), 8.38 (s, 1H). [M + H]<sup>+</sup> 511.3.

**Phenyl N-[1-[8-(2-Chlorophenyl)-9-(4-chlorophenyl)-9H-purin-6-yl]piperidin-4-yl]carbamate (**7**).** The reaction proceeded in 50% yield.

$^1\text{H}$  NMR (300 MHz,  $\text{CDCl}_3$ )  $\delta$  1.59–1.72 (m, 2H), 2.22 (d,  $J = 11.40$  Hz, 2H), 3.37 (t,  $J = 12.10$  Hz, 2H), 3.84–4.02 (m, 1H), 4.99 (d,  $J = 7.72$  Hz, 1H), 5.45 (br s, 2H), 7.02–7.45 (m, 12H), 7.52 (d,  $J = 6.88$  Hz, 1H), 8.40 (s, 1H).  $[\text{M} + \text{H}]^+ 559.8$ .

**General Procedure for Making Amides from 1-[8-(2-Chlorophenyl)-9-(4-chlorophenyl)-9H-purin-6-yl]piperidin-4-amine (4) Using Carboxylic Acids.** To a solution of 1-[8-(2-chlorophenyl)-9-(4-chlorophenyl)-9H-purin-6-yl]piperidin-4-amine (4) (22 mg, 0.05 mmol, 1 equiv) in 2 mL of THF were added triethylamine (0.02 mL, 0.143 mmol, 3 equiv), (benzotriazol-1-yloxy)tris(dimethylamino)phosphonium hexafluorophosphate (BOP) (22 mg, 0.05 mmol, 1 equiv), and the appropriate carboxylic acid (1 equiv). The reaction was stirred for 16 h. The reaction was concentrated in vacuo. The crude material was purified by silica gel column chromatography using 0–100% ethyl acetate/hexane to yield the compound. The product was purified further by dissolving in ethyl acetate and precipitating with hexane. The solid, pure compound was collected.

*N*-{1-[8-(2-Chlorophenyl)-9-(4-chlorophenyl)-9H-purin-6-yl]piperidin-4-yl}cyclohexanecarboxamide (8). The reaction proceeded in >99% yield.  $^1\text{H}$  NMR (300 MHz,  $\text{CDCl}_3$ )  $\delta$  1.15–2.17 (m, 14H), 2.23–2.40 (m, 1H), 3.31 (t,  $J = 12.20$  Hz, 2H), 4.05–4.25 (m, 1H), 5.22–5.61 (m, 3H), 7.14–7.42 (m, 7H), 7.51 (d,  $J = 6.69$  Hz, 1H), 8.38 (s, 1H).  $[\text{M} + \text{H}]^+ 549.5$ .

*N*-{1-[8-(2-Chlorophenyl)-9-(4-chlorophenyl)-9H-purin-6-yl]piperidin-4-yl}pentanamide (9). The reaction proceeded in >99% yield.  $^1\text{H}$  NMR (300 MHz,  $\text{CDCl}_3$ )  $\delta$  0.84–0.98 (m, 3H), 1.27–1.75 (m, 5H), 2.05–2.23 (m, 3H), 2.26–2.44 (m, 1H), 3.31 (t,  $J = 12.24$  Hz, 2H), 4.02–4.30 (m, 1H), 5.22–5.63 (m, 3H), 7.13–7.44 (m, 7H), 7.51 (d,  $J = 6.78$  Hz, 1H), 8.38 (s, 1H).  $[\text{M} + \text{H}]^+ 523.5$ .

*N*-{1-[8-(2-Chlorophenyl)-9-(4-chlorophenyl)-9H-purin-6-yl]piperidin-4-yl}-2-cyclohexylacetamide (10). The reaction proceeded in >99% yield.  $^1\text{H}$  NMR (300 MHz,  $\text{CDCl}_3$ )  $\delta$  0.86–1.00 (m, 3H), 1.05–1.87 (m, 10H), 2.02–2.18 (m, 4H), 3.31 (t,  $J = 12.10$  Hz, 2H), 4.10–4.28 (m, 1H), 5.22–5.62 (m, 3H), 7.14–7.43 (m, 7H), 7.51 (d,  $J = 6.78$  Hz, 1H), 8.38 (s, 1H).  $[\text{M} + \text{H}]^+ 562.2$ .

*N*-{1-[8-(2-Chlorophenyl)-9-(4-chlorophenyl)-9H-purin-6-yl]piperidin-4-yl}-3-methylbutanamide (11). The reaction proceeded in >99% yield.  $^1\text{H}$  NMR (300 MHz,  $\text{CDCl}_3$ )  $\delta$  0.97 (dd,  $J = 9.94$ , 6.45 Hz, 6H), 1.50 (qd,  $J = 11.85$ , 3.81 Hz, 1H), 2.01–2.17 (m, 4H), 2.19–2.27 (m, 2H), 3.31 (t,  $J = 12.24$  Hz, 2H), 4.10–4.27 (m, 1H), 5.39 (d,  $J = 8.01$  Hz, 3H), 7.14–7.42 (m, 7H), 7.51 (d,  $J = 6.78$  Hz, 1H), 8.38 (s, 1H).  $[\text{M} + \text{H}]^+ 523.3$ .

*N*-{1-[8-(2-Chlorophenyl)-9-(4-chlorophenyl)-9H-purin-6-yl]piperidin-4-yl}cyclopentanecarboxamide (12). The reaction proceeded in 86% yield.  $^1\text{H}$  NMR (300 MHz,  $\text{CDCl}_3$ )  $\delta$  1.39–1.99 (m, 9H), 2.06–2.21 (m, 3H), 2.41–2.58 (m, 1H), 3.31 (t,  $J = 12.24$  Hz, 2H), 4.08–4.27 (m, 1H), 5.40 (d,  $J = 7.91$  Hz, 3H), 7.12–7.42 (m, 7H), 7.51 (d,  $J = 6.78$  Hz, 1H), 8.38 (s, 1H).  $[\text{M} + \text{H}]^+ 535.5$ .

*N*-{1-[8-(2-Chlorophenyl)-9-(4-chlorophenyl)-9H-purin-6-yl]piperidin-4-yl}-4-methylpentanamide (13). The reaction proceeded in 82% yield.  $^1\text{H}$  NMR (300 MHz,  $\text{CDCl}_3$ )  $\delta$  0.85–0.95 (m, 6H), 1.40–1.62 (m, 5H), 2.03–2.23 (m, 3H), 2.34 (t,  $J = 7.54$  Hz, 1H), 3.31 (t,  $J = 12.24$  Hz, 2H), 4.08–4.29 (m, 1H), 5.42 (d,  $J = 7.91$  Hz, 3H), 7.14–7.43 (m, 7H), 7.51 (d,  $J = 7.16$  Hz, 1H), 8.38 (s, 1H).  $[\text{M} + \text{H}]^+ 537.5$ .

*N*-{1-[8-(2-Chlorophenyl)-9-(4-chlorophenyl)-9H-purin-6-yl]piperidin-4-yl}-2-cyclopentylacetamide (14). The reaction proceeded in 98% yield.  $^1\text{H}$  NMR (300 MHz,  $\text{CDCl}_3$ )  $\delta$  1.06–1.23 (m, 3H), 1.44–1.69 (m, 5H), 1.74–1.93 (m, 3H), 2.06–2.28 (m, 3H), 2.30–2.41 (m, 1H), 3.32 (t,  $J = 12.20$  Hz, 2H), 4.08–4.29 (m, 1H), 5.41 (d,  $J = 7.91$  Hz, 3H), 7.14–7.42 (m, 7H), 7.51 (d,  $J = 6.78$  Hz, 1H), 8.38 (s, 1H).  $[\text{M} + \text{H}]^+ 549.5$ .

**General Procedure for Making Amides from 1-[8-(2-Chlorophenyl)-9-(4-chlorophenyl)-9H-purin-6-yl]piperidin-4-amine (4) Using Amino Acids.** To a solution of 1-[8-(2-chlorophenyl)-9-(4-chlorophenyl)-9H-purin-6-yl]piperidin-4-amine (4) (22 mg, 0.05 mmol, 1 equiv) in 2 mL of THF were added triethylamine (0.02 mL, 0.143 mmol, 3 equiv), (benzotriazol-1-yloxy)tris(dimethylamino)phosphonium hexafluorophosphate (BOP) (22 mg, 0.05 mmol, 1 equiv), and the appropriate carboxylic acid (1

equiv). The reaction was stirred for 16 h. The reaction was concentrated in vacuo. The crude material was purified by silica gel column chromatography using 0–100% CMA 80/dichloromethane to yield the compound. The product was purified further by dissolving in ethyl acetate, washing with water, and precipitating with hexane. The solid, pure compound was collected.

*N*-{1-[8-(2-Chlorophenyl)-9-(4-chlorophenyl)-9H-purin-6-yl]piperidin-4-yl}-3-(piperidin-1-yl)propanamide (15). The reaction proceeded in 41% yield.  $^1\text{H}$  NMR (300 MHz,  $\text{CDCl}_3$ )  $\delta$  1.52–1.60 (m, 4H), 1.80 (br s, 3H), 1.98–2.14 (m, 3H), 2.76 (t,  $J = 5.93$  Hz, 2H), 2.93 (br s, 2H), 3.30 (br s, 2H), 3.40 (br s, 2H), 3.56 (br s, 2H), 3.97–4.15 (m, 1H), 5.36–5.59 (m, 2H), 6.46–6.65 (m, 1H), 7.15–7.42 (m, 7H), 7.54 (d,  $J = 7.63$  Hz, 1H), 8.37 (s, 1H).  $[\text{M} + \text{H}]^+ 580.6$ .

*N*-{1-[8-(2-Chlorophenyl)-9-(4-chlorophenyl)-9H-purin-6-yl]piperidin-4-yl}-2-(dimethylamino)acetamide (16). The reaction proceeded in 11% yield.  $^1\text{H}$  NMR (300 MHz,  $\text{CDCl}_3$ )  $\delta$  1.50–1.66 (m, 2H), 2.01–2.13 (m, 2H), 2.48 (s, 7H), 2.64 (d,  $J = 9.32$  Hz, 1H), 3.36 (t,  $J = 11.82$  Hz, 2H), 4.05–4.26 (m, 1H), 5.41 (br s, 2H), 7.08 (d,  $J = 8.19$  Hz, 1H), 7.14–7.42 (m, 7H), 7.51 (d,  $J = 6.78$  Hz, 1H), 8.37 (s, 1H).  $[\text{M} + \text{H}]^+ 524.7$ .

*N*-{1-[8-(2-Chlorophenyl)-9-(4-chlorophenyl)-9H-purin-6-yl]piperidin-4-yl}aminosulfonamide (17). To a solution of 1-[8-(2-chlorophenyl)-9-(4-chlorophenyl)-9H-purin-6-yl]piperidin-4-amine (4) (36.6 mg, 0.083 mmol, 1 equiv) in 2 mL of dioxane was added sulfamide (40 mg, 0.42 mmol, 5 equiv). The reaction was heated at 80 °C for 16 h. The reaction was concentrated in vacuo. The crude material was purified by silica gel column chromatography using 0–100% ethyl acetate/hexane to yield 34 mg (79%) of the desired compound.  $^1\text{H}$  NMR (300 MHz,  $\text{MeOH}-d_4$ )  $\delta$  1.51–1.72 (m, 2H), 2.15 (br s, 2H), 3.38–3.52 (m, 2H), 3.54–3.65 (m, 1H), 5.18–5.41 (m, 2H), 7.24–7.50 (m, 7H), 7.54–7.67 (m, 1H), 8.23 (s, 1H).  $[\text{M} + \text{H}]^+ 518.5$ .

*N*-{1-[8-(2-Chlorophenyl)-9-(4-chlorophenyl)-9H-purin-6-yl]piperidin-4-yl}-1,1,1-trifluoromethanesulfonamide (18). To a solution of 1-[8-(2-chlorophenyl)-9-(4-chlorophenyl)-9H-purin-6-yl]piperidin-4-amine (4) (27.9 mg, 0.064 mmol, 1 equiv) in 2 mL of dichloromethane were added triethylamine (0.027 mL, 0.191 mmol, 3 equiv) and the trifluoromethanesulfonic anhydride (0.01 mL, 0.069 mmol, 1 equiv). The reaction was stirred for 16 h. The reaction was concentrated in vacuo. The crude material was purified by silica gel column chromatography using 0–100% ethyl acetate/hexane to yield 9 mg (25%) of the desired compound.  $^1\text{H}$  NMR (300 MHz,  $\text{CDCl}_3$ )  $\delta$  1.60–1.76 (m, 2H), 2.20 (d,  $J = 12.62$  Hz, 2H), 3.30 (t,  $J = 12.57$  Hz, 2H), 3.71–3.92 (m, 1H), 4.95 (d,  $J = 8.48$  Hz, 1H), 5.50 (d,  $J = 12.34$  Hz, 2H), 7.14–7.43 (m, 7H), 7.50 (d,  $J = 6.97$  Hz, 1H), 8.39 (s, 1H).  $[\text{M} + \text{H}]^+ 571.7$ .

**Calcium Mobilization and Radioligand Displacement Assays.** Each compound was pharmacologically characterized using a functional fluorescent CB1-activated  $\text{G}\alpha_{q16}$ -coupled intracellular calcium mobilization assay in CHO-K1 cells, as has been described in our previous publication, and the apparent antagonist dissociation equilibrium constant ( $K_e$ ) values were determined.<sup>13</sup> Briefly, CHO-K1 cells were engineered to coexpress human CB1 and  $\text{G}\alpha_{q16}$ . Activation of CB1 by an agonist then leads to the generation of inositol phosphatase 3 (IP3) and activation of IP3 receptors, which leads to the mobilization of intracellular calcium. Calcium flux was monitored in a 96-well format using the fluorescent dye Calcein-4 AM in an automated plate reader (Flexstation, Molecular Devices). The  $K_e$  of a test compound was measured by its ability to shift the concentration response curve of the synthetic CB1 agonist CP55940 to the right using the equation

$K_e = [\text{ligand}]/[\text{DR} - 1]$  where DR is the  $\text{EC}_{50}$  ratio of CP55940 in the presence or absence of a test agent.

Typically, three different antagonist concentrations were used to shift a five-point CP55940 agonist curve (10, 1, 0.1, 0.01, and 0.001  $\mu\text{M}$ ). The data were fitted using nonlinear regression analyses (GraphPad Prism). The  $K_e$  values were used to calculate  $\text{pA}_2$ , which is the negative logarithm of  $K_e$ .<sup>19</sup>

Further characterization of select compounds was performed using radioligand displacement of [ $^3\text{H}$ ]SR141716, and the equilibrium

dissociation constant ( $K_i$ ) values were determined as described previously.<sup>13</sup> The selectivity of these compounds at CB1 versus CB2 was also determined by obtaining  $K_i$  values of either receptor using the displacement of [<sup>3</sup>H]CP55940 in the membranes of CHO-K1 cells overexpressing either receptor. The data reported are the average values from 3 to 6 measurements performed in duplicate. The standard errors for most measurements were between 5 and 25% of the mean and have been left out from the tables and figures for clarity.

**Pharmacokinetic Studies.** Male Sprague–Dawley (SD) rats, aged 9 weeks at the time of dosing, were acquired from Charles River Laboratories and were dosed orally. Doses were formulated in corn oil and administered by gavage. Animals were sacrificed at various time points and analyzed. Samples were prepared and analyzed as follows. Plasma (50  $\mu$ L) was mixed with 300  $\mu$ L of acetonitrile, vortexed, and centrifuged at 9000g for 5 min. The supernatant was transferred to autosampler vials with low-volume inserts and injected without dilution. The brain was homogenized with 50:50 ethanol/water (3:1, v/v) using a Potter Elvehjem type homogenizer. The homogenate (50  $\mu$ L) was mixed with 300  $\mu$ L of acetonitrile, vortexed, and centrifuged at 9000g for 5 min. This supernatant was transferred to autosampler vials with low-volume inserts and injected without dilution. Standards were prepared as above for each compound in blank plasma, blank liver homogenate, and blank brain homogenate. The standards used were within 15% of nominal except for 20% at LOQ. Compounds for LC–MS/MS analyses were supplied at 1 mg/mL in methanol. The stock solutions were further diluted to  $\sim$ 100 ng/mL. The 100 ng/mL solutions were used to optimize the mass spectrometer for MRM transitions and mass spectrometer parameters. Infusion and flow injection optimization were also performed. LC–MS/MS was conducted using an Applied Biosystems API 4000 coupled with an Agilent 1100 HPLC system. Chromatography was performed with a Phenomenex Luna C18 (50  $\times$  2 mm, 5  $\mu$ m) column. Mobile phases were 0.1% formic acid and 10 mM ammonium formate in water (A) and 0.1% formic acid and 10 mM ammonium formate in methanol (B). The initial conditions were 10% B and held for 1 min followed by a linear gradient to 90% B over 5 min. Ninety percent B was held for 2 min before returning to the initial conditions. Compound 9 was analyzed with multiple reactions and was monitored in the positive mode with a transition of 522.922  $\rightarrow$  368.0. The following parameters were used, DP = 171, CE = 51, and CXP = 30.

**Tetrad Test.** Male adult ICR mice, obtained from Harlan (Indianapolis, IN) and housed singly in polycarbonate mouse cages, were used for the assessment of locomotor suppression, antinociception, hypothermia, and catalepsy. Separate mice were used for testing each condition in this battery of procedures. All animals were maintained in a temperature-controlled (20–22  $^{\circ}$ C) environment with a 12 h light–dark cycle (lights on at 6 a.m.) and had free access to food and water when in their home cages. The in vivo studies reported in this Article were carried out in accordance with guidelines published in the Guide for the Care and Use of Laboratory Animals (National Research Council, 2011).  $\Delta^9$ -Tetrahydrocannabinol ( $\Delta^9$ -THC), obtained from the National Institute on Drug Abuse (NIDA, Bethesda, MD) through the NIDA Drug Supply Program, was mixed in a vehicle of 7.8% polysorbate 80 N.F. (VWR, Marietta, GA) and 92.2% sterile saline USP (Butler Schein, Dublin, OH) and was given by i.v. injection. Compound 9 was dissolved in peanut oil and administered via oral gavage at a volume of 5 mL/kg.

The measurement of spontaneous activity occurred in standard Plexiglas locomotor activity chambers (33  $\times$  51  $\times$  23 cm<sup>3</sup>). Beam breaks were recorded by San Diego Instruments Photobeam Activity System software (model SDI: V-71215, San Diego, CA) on a computer located in the experimental room. The apparatus contained two 4-beam infrared arrays that measured horizontal movement. A glass beaker filled with water heated at 55  $^{\circ}$ C was used for the warm-water tail-withdrawal procedure. A digital thermometer (Physitemp Instruments, Inc., Clifton, NJ) was used to measure rectal temperature. The ring immobility device consisted of an elevated metal ring (5.5 cm diameter, 16 cm height) attached to a metal stand.

Each mouse was tested in a battery of four tests in which cannabinoid agonists produced a characteristic profile of in vivo

effects:<sup>20</sup> suppression of locomotor activity, antinociception, decreased rectal temperature, and ring immobility. Prior to injection, rectal temperature and baseline latency in the warm-water tail-withdrawal test were measured in the mice. The latter procedure involved immersing the mouse's tail into a water bath maintained at 55  $^{\circ}$ C and recording latency (s) for tail removal. Control latencies were 1–3 s. A 10 s maximal latency was used to avoid damage to the mouse's tail. After measurement of the temperature and baseline tail-withdrawal latency, the mice were dosed with vehicle or with 10 mg/kg 9 via oral gavage. Thirty minutes later, mice were injected i.v. in the tail vein with vehicle or with 30 mg/kg  $\Delta^9$ -THC. After 5 min, they were placed into individual activity chambers for 10 min. Spontaneous activity was measured as the total number of beam interruptions during the entire session. Tail-withdrawal latency was measured again at 20 min postinjection. Rectal temperature was measured again at 30 min postinjection. At 40 min postinjection, the mice were placed on the elevated ring apparatus, and the amount of time that the animals remained motionless during a 5 min period was recorded.

Rectal temperature values were expressed as the difference between the control temperature (before injection) and the temperature following drug administration ( $\Delta$   $^{\circ}$ C). Spontaneous activity was measured as total number of photocell beam interruptions during the 10 min session. Antinociception was expressed as the percent maximum possible effect (MPE) using a 10 s maximum test latency as follows: ((test – control)/(10 – control))  $\times$  100. During the assessment for catalepsy, the total amount of time (s) that the mouse remained motionless on the ring apparatus (except for breathing and whisker movement) was measured and was used as an indication of catalepsy-like behavior. This value was divided by 300 s and multiplied by 100 to obtain a percent immobility. Factorial ANOVAs ( $\Delta^9$ -THC dose  $\times$  9 dose) were used to analyze the results of the tetrad tests. Significant main effects and interactions were further analyzed with Tukey post hoc tests ( $\Delta$  = 0.05) as necessary.

## ■ ASSOCIATED CONTENT

### ● Supporting Information

HPLC and melting point data of target compounds 5–18. This material is available free of charge via the Internet at <http://pubs.acs.org>.

## ■ AUTHOR INFORMATION

### Corresponding Author

\*Tel: 919-541-6795. Fax: 919-541-8868. E-mail: [rmaitra@rti.org](mailto:rmaitra@rti.org).

### Notes

The authors declare no competing financial interest.

## ■ ACKNOWLEDGMENTS

The authors thank Anne Gilliam for performing the radioligand displacement assays. We express our gratitude to the NIDA drug supply program for providing radiolabeled probes and to Dr. Brian Thomas for supplying the CB1 cells. This research was funded by research grants AA019740-01 to R.M. and DA-003672 to J.W.

## ■ ABBREVIATIONS USED

CB1, cannabinoid receptor 1; CB2, cannabinoid receptor 2; CMA 80, 80% chloroform, 18% methanol, and 2% ammonium hydroxide; CNS, central nervous system; BBB, blood-brain barrier; TPSA, topological polar surface area; ECS, endocannabinoid system; CBR, cannabinoid receptors;  $K_e$ , apparent affinity constant; MDCK-mdr1, Madin-Darby canine kidney cells transfected with the human MDR1 gene; A, apical; B, basal; BOP, benzotriazole-1-yl-oxytris(dimethylamino)-phosphonium hexafluorophosphate; CHO-K1, chinese hamster

ovary cells; IP<sub>3</sub>, inositol phosphatase 3; MRM, multiple reaction monitoring; LOQ, below the limit of quantitation; NA, not applicable

## REFERENCES

- (1) Pertwee, R. G.; Howlett, A. C.; Abood, M. E.; Alexander, S. P.; Di Marzo, V.; Elphick, M. R.; Greasley, P. J.; Hansen, H. S.; Kunos, G.; Mackie, K.; Mechoulam, R.; Ross, R. A. International Union of Basic and Clinical Pharmacology. LXXIX. Cannabinoid receptors and their ligands: Beyond CB<sub>1</sub> and CB<sub>2</sub>. *Pharmacol. Rev.* **2010**, *62*, 588–631.
- (2) Bouaboula, M.; Bianchini, L.; McKenzie, F. R.; Pouyssegur, J.; Casellas, P. Cannabinoid receptor CB<sub>1</sub> activates the Na<sup>+</sup>/H<sup>+</sup> exchanger NHE-1 isoform via Gi-mediated mitogen activated protein kinase signaling transduction pathways. *FEBS Lett.* **1999**, *449*, 61–65.
- (3) Bouaboula, M.; Perrachon, S.; Milligan, L.; Canat, X.; Rinaldi-Carmona, M.; Portier, M.; Barth, F.; Calandra, B.; Pecceu, F.; Lupker, J.; Maffrand, J. P.; Le Fur, G.; Casellas, P. A selective inverse agonist for central cannabinoid receptor inhibits mitogen-activated protein kinase activation stimulated by insulin or insulin-like growth factor 1. Evidence for a new model of receptor/ligand interactions. *J. Biol. Chem.* **1997**, *272*, 22330–22339.
- (4) Janero, D. R.; Makriyannis, A. Cannabinoid receptor antagonists: Pharmacological opportunities, clinical experience, and translational prognosis. *Expert Opin. Emerging Drugs* **2009**, *14*, 43–65.
- (5) Di Marzo, V. CB<sub>1</sub> receptor antagonism: Biological basis for metabolic effects. *Drug Discovery Today* **2008**, *13*, 1026–1041.
- (6) Lee, H. K.; Choi, E. B.; Pak, C. S. The current status and future perspectives of studies of cannabinoid receptor 1 antagonists as anti-obesity agents. *Curr. Top. Med. Chem.* **2009**, *9*, 482–503.
- (7) Chugh, B. P.; Lerch, J. P.; Yu, L. X.; Pienkowski, M.; Harrison, R. V.; Henkelman, R. M.; Sled, J. G. Measurement of cerebral blood volume in mouse brain regions using micro-computed tomography. *NeuroImage* **2009**, *47*, 1312–1318.
- (8) Edvinsson, L.; Nielsen, K. C.; Owman, C. Circadian rhythm in cerebral blood volume of mouse. *Experientia* **1973**, *29*, 432–3.
- (9) Kunos, G.; Tam, J. The case for peripheral CB<sub>1</sub> receptor blockade in the treatment of visceral obesity and its cardiometabolic complications. *Br. J. Pharmacol.* **2011**, *163*, 1423–1431.
- (10) Fulp, A.; Bortoff, K.; Zhang, Y.; Seltzman, H.; Mathews, J.; Snyder, R.; Fennell, T.; Maitra, R. Diphenyl purine derivatives as peripherally selective cannabinoid receptor 1 antagonists. *J. Med. Chem.* **2012**, *55*, 10022–10032.
- (11) Griffith, D. A.; Hadcock, J. R.; Black, S. C.; Iredale, P. A.; Carpino, P. A.; DaSilva-Jardine, P.; Day, R.; DiBrino, J.; Dow, R. L.; Landis, M. S.; O'Connor, R. E.; Scott, D. O. Discovery of 1-[9-(4-chlorophenyl)-8-(2-chlorophenyl)-9H-purin-6-yl]-4-ethylaminopiperidine-4-carboxylic acid amide hydrochloride (CP-945,598), a novel, potent, and selective cannabinoid type 1 receptor antagonist. *J. Med. Chem.* **2009**, *52*, 234–237.
- (12) Fulp, A.; Bortoff, K.; Seltzman, H.; Zhang, Y.; Mathews, J.; Snyder, R.; Fennell, T.; Maitra, R. Design and synthesis of cannabinoid receptor 1 antagonists for peripheral selectivity. *J. Med. Chem.* **2012**, *55*, 2820–2834.
- (13) Zhang, Y.; Gilliam, A.; Maitra, R.; Damaj, M. I.; Tajuba, J. M.; Seltzman, H. H.; Thomas, B. F. Synthesis and biological evaluation of bivalent ligands for the cannabinoid 1 receptor. *J. Med. Chem.* **2010**, *53*, 7048–7060.
- (14) Wiley, J. L.; Martin, B. R. Cannabinoid pharmacological properties common to other centrally acting drugs. *Eur. J. Pharmacol.* **2003**, *471*, 185–193.
- (15) Compton, D. R.; Aceto, M. D.; Lowe, J.; Martin, B. R. In vivo characterization of a specific cannabinoid receptor antagonist (SR141716A): Inhibition of delta 9-tetrahydrocannabinol-induced responses and apparent agonist activity. *J. Pharmacol. Exp. Ther.* **1996**, *277*, 586–594.
- (16) Leite, C. E.; Mocelin, C. A.; Petersen, G. O.; Leal, M. B.; Thiesen, F. V. Rimonabant: An antagonist drug of the endocannabinoid system for the treatment of obesity. *Pharmacol. Rep.* **2009**, *61*, 217–224.
- (17) Liu, J.; Zhou, L.; Xiong, K.; Godlewski, G.; Mukhopadhyay, B.; Tam, J.; Yin, S.; Gao, P.; Shan, X.; Pickel, J.; Batailler, R.; O'Hare, J.; Scherer, T.; Buettner, C.; Kunos, G. Hepatic cannabinoid receptor-1 mediates diet-induced insulin resistance via inhibition of insulin signaling and clearance in mice. *Gastroenterology* **2012**, *142*, 1218–1228.
- (18) Tam, J.; Cinar, R.; Liu, J.; Godlewski, G.; Wesley, D.; Jourdan, T.; Szanda, G.; Mukhopadhyay, B.; Chedester, L.; Liow, J. S.; Innis, R. B.; Cheng, K.; Rice, K. C.; Deschamps, J. R.; Chorvat, R. J.; McElroy, J. F.; Kunos, G. Peripheral cannabinoid-1 receptor inverse agonism reduces obesity by reversing leptin resistance. *Cell Metab.* **2012**, *16*, 167–179.
- (19) Arunlakshana, O.; Schild, H. O. Some quantitative uses of drug antagonists. *Br. J. Pharmacol. Chemother.* **1959**, *14*, 48–58.
- (20) Martin, B. R.; Compton, D. R.; Thomas, B. F.; Prescott, W. R.; Little, P. J.; Razdan, R. K.; Johnson, M. R.; Melvin, L. S.; Mechoulam, R.; Ward, S. J. Behavioral, biochemical, and molecular modeling evaluations of cannabinoid analogs. *Pharmacol., Biochem. Behav.* **1991**, *40*, 471–478.